BNL-42550
Conf-8909160--1
Received by OSTI
SEP 19 1989

GLANCING ANGLE X-RAY STUDIES OF OXIDE FILMS

A. J. Davenport and H. S. Isaacs

Brookhaven National Laboratory, Upton, NY 11973, USA

BNL--42550
DE89 017828

ABSTRACT

High brightness synchrotron radiation incident at glancing angles has been used to study inhibiting species present in low concentrations in oxide films on aluminum. Glancing incident angle fluorescence measurements give surface-sensitive information on the valence state of elements from the shape of the x-ray absorption edge. Angle-resolved measurements show the depth distribution of the species present.

INTRODUCTION: X-RAY ABSORPTION MEASUREMENTS

The absorption of x-rays by materials typically decreases as the incident x-ray energy is increased. However, there is a sudden increase in the absorption when the x-rays have just sufficient energy to promote a core electron to an unoccupied valence level or to the continuum. The position of this x-ray "edge" is characteristic of the element involved: this confers clear element specificity because the energies of the absorption edges for different elements are well spaced. The structure of the absorption edge (XANES or X-ray Absorption Near Edge Structure) is composed of a number of discrete absorption bands super-imposed on the step due to transition of the core electron to the continuum. The bands are due to transitions of core electrons to bound valence levels. The relative intensities of these bands are affected by the valency of the central atom and the co-ordination symmetry. There is a general trend for absorption edge features to move to higher energies as the central atom become more positively charged (i.e. has a higher valency).

INCORPORATION OF CHROMATE IN ANODIC OXIDE FILMS ON ALUMINUM

Chromates are very effective corrosion inhibitors for aluminum and its alloys. The mechanism of inhibition involves incorporation of chromium into the oxide film with reduction of some or all of the 6-valent chromium (CrO_4^{2-}) to the 3-valent state (Cr_2O_3). This has been determined from XPS measurements (1,2). XANES measurements (3) have also been used to determine the valence state of chromium in oxide films on aluminum. XANES is particularly well-suited to distinguishing between 3-valent and 6-valent chromium species because of the distinctive appearance of the Cr(VI) spectrum. It is characterized by the appearance of a large peak just below the absorption edge, referred to as the "pre-edge peak", as shown in Fig. 1.

The ratio of the pre-edge peak height to the edge height in a mixed sample gives the ratio of the Cr VI to the total chromium present in the sample. This method for making a semi-quantitative estimate of the Cr III:Cr VI ratio has been used to investigate the interaction of chromate with oxide films grown on aluminum (3). Both the air-formed film and films grown by anodizing electropolished aluminum substrates were exposed to a chromate solution. Ex situ XANES measurements were made at the chromium edge by measuring the fluorescent signal with the x-rays incident at very small glancing angles in order to give surface sensitivity (4). The experimental arrangement is shown in Fig. 2. The results showed that in the air-formed film, Cr III predominates, but as the thickness of the oxide film increased by anodizing, the proportion of Cr VI increases until for a 36 nm anodic oxide film, only Cr VI is found. The distribution of chromium in anodic

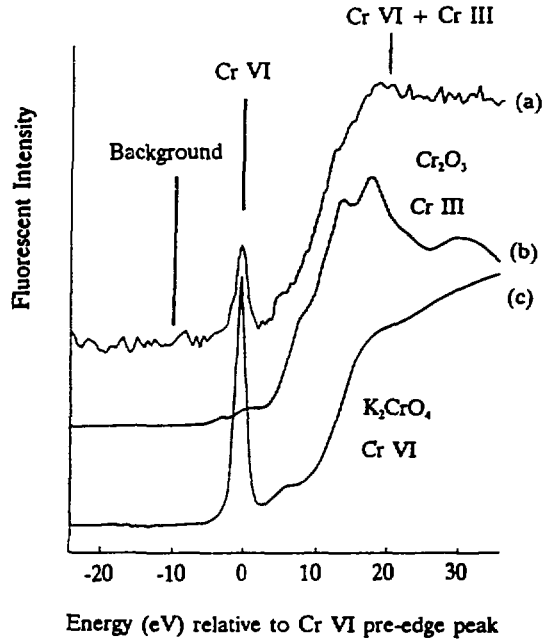

Fig. 1. X-ray absorption edges plotted relative to the Cr VI pre-edge peak. (a) Aluminum film anodized 100 V in 0.1 M K_2CrO_4 [fluorescent intensity (I_f/I_0)]. (b) Cr_2O_3 (Cr III) powder measured in transmission [$\ln(I_0/I)$]. (c) K_2CrO_4 (Cr VI) powder (transmission).

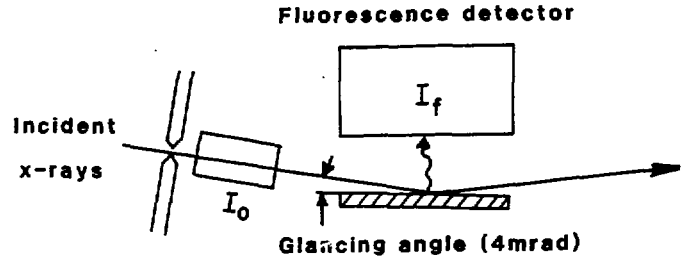

Fig. 2. Experimental arrangement for the detection of fluorescent x-rays form surface layers [after Heald et al. (4)].

oxide films grown on aluminum in chromate solutions has been determined by SIMS (5). It was determined that chromium was present in significant concentrations only in the outer 15 nm of a 75 nm film. However, SIMS can give no information on the valence state of the species present.

In order to investigate the distributions of Cr III and Cr VI in anodic oxide films on aluminum, the angular dependence of the x-ray fluorescence was measured at very small glancing angles (a few mrad) (6). The index of refraction of x-rays is slightly less than 1 so at small incident angles, total external reflection can occur with very small penetration of x-rays into the surface (a few nm). As the incident angle increases to the critical angle, the penetration depth of the x-rays increases by over an order of magnitude. This can be calculated from the Fresnel equations (7). As the incident angle and the penetration depth increase, the x-ray intensity in the material at a particular depth increases. The fluorescent signal is then the product of the x-ray intensity and the concentration of the fluorescing species integrated over the thickness of the film.

The absorption edge from the chromium in the oxide film measured at an incident x-ray angle of 4 mrad (below the critical angle at 6 mrad) is shown in Fig. 1. It shows the characteristic pre-edge peak of Cr VI. The ratio of the pre-peak height to the edge height is approximately 1:3, suggesting a Cr VI:Cr III ratio of 1:2 in the sample. RBS measurements were carried out which indicated that chromium is present in sub-monolayer amounts (8). Fluorescence measurements were made with varying angle at the energies indicated in Fig. 1. At -10 eV (with respect to the pre-edge peak), the signal gave the background fluorescence. At the pre-edge peak, Cr VI atoms absorb x-rays and fluoresces whereas Cr III do not. The difference between the curve at 0 eV and that at -10 eV gives the

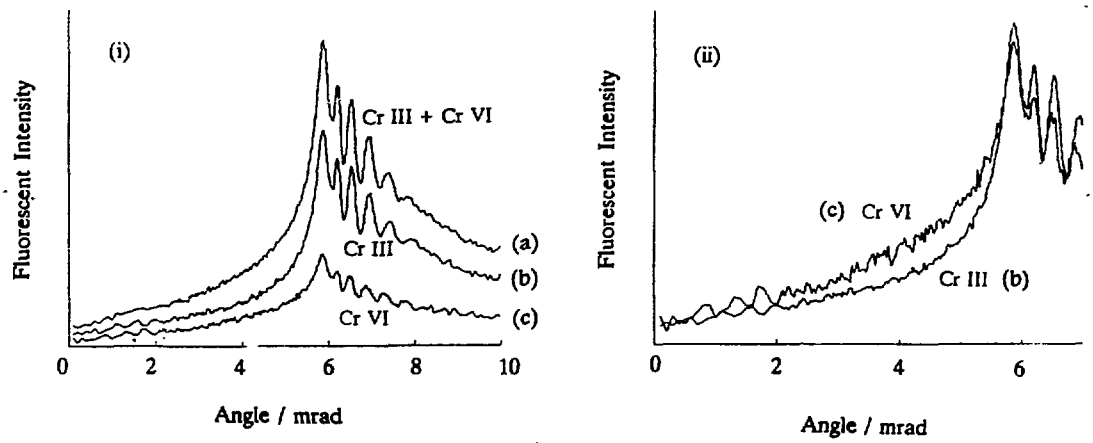

Fig. 3(i). Angle-dependence of the fluorescent intensity at constant energy for an aluminum film anodized to 100 V in 0.1 M K_2CrO_4. The curves give the difference between curves measured at different energies:
(a) +20 eV - -10 eV, (b) +10 eV - 0 eV,
(c) 0 eV - -10 eV (6).

(ii) Curves (b) and (c) from Fig. 3(i) have been normalized to give the same maximum value at the critical angle (6).

fluorescent signal due to Cr VI atoms. This is curve (c) in Fig. 3(i). At +20 eV, at the top of the edge, both Cr VI and Cr III are fluorescing. Curve (a) in Fig. 3 shows the data recorded at +20 eV with the -10 eV background subtracted. The difference between the +20 eV and -0 eV curves gives the signal due to Cr III [curve (b) in Fig. 3]. All the curves increase smoothly up to the critical angle where large oscillations begin. These occur because the x-rays have now penetrated as far as the metal/oxide and metal/substrate interfaces and standing waves are set up in the material. It is the region below the critical angle which is of interest for determination of the chromium distribution. In Fig. 3(ii), curves (b) (Cr III) and (c) (Cr VI) from Fig. 3(i) are shown normalized to give the same maximum value at the critical angle. The curve for Cr VI is shallower than that for Cr III. This indicates that more Cr VI is found closer to the surface whereas Cr III is more uniformly distributed. Deconvolution of these curves gives the depth distribution of the chromium species. However, this requires a detailed knowledge of the x-ray intensity with depth as a function of incident angle, which is a sensitive function of the oxide density.

VALENCE STATE OF CERIUM IN OXIDE FILMS ON ALUMINUM

Although chromates are successful corrosion inhibitors for aluminum and its alloys, there is considerable interest in their replacement due to their toxicity. It has recently been shown that rare earth cations, particularly cerium ions, can confer corrosion resistance comparable with chromates (9-11). They can either be added to aqueous environments in low concentrations (100-1000 ppm) (9,10) or they can be incorporated in the passive film prior to exposure to a corrosive environment (9-11). Cerium is thought to act as a cathodic inhibitor: at sites on the surface where the cathodic reaction (oxygen reduction) predominates, the local pH increases to the point where cerium hydroxide can precipitate on the surface. This forms a film with low electronic conductivity which stifles the oxygen reduction reaction (9,10).

The film formed on immersion of 7075 aluminum alloy in a solution of 200 ppm $CeCl_3$ in 0.1 M NaCl for 20 days has been investigated using Auger and XPS (12). It was found to be approximately 140 nm in thickness and to consist almost entirely of cerium oxides and hydroxides with very little aluminum oxide. From the relative amounts of cerium and oxygen present, it was inferred that cerium is present in both the +3 ard +4 valence states although no direct measurements of the valence states were made.

Clear distinction can be made between the +3 and +4 valence states of cerium from XANES measurements at both the Ce L1 edge and the Ce L3 edge (13,14). The L3 edge is more frequently used in experiments as it is more intense than the L1 edge. The edges are shown in Fig. 4 for CeO_2 (Ce IV) and $CeCl_3 \cdot 7H_2O$ (Ce III). The Ce L3 edge for a number of oxide films measured in fluorescence geometry with an incident angle of 4 mrad is shown in Fig. 4. The cerium-containing films were grown on both aluminum films evaporated onto float glass substrates and polished pieces of aluminum Alloy 5052 by galvanostatic cathodizing in an alkaline solution of 0.1 M $CeCl_3$ for 30 min at 10 μAcm^{-2}. Some of the specimens treated in this way were immersed in a solution of NaCl for a week. Comparison of the data from aluminum evaporated onto glass with that from the Alloy 5052 shows that the type of aluminum substrate is not critical in determining the behavior of the cerium. The freshly formed film [curves (a) and (b)] contains predominantly 3-valent cerium: the main peak is consistent with 3-valent cerium [curve (f)]. However, the peak is broader than that of

$CeCl_3$ and extends over the first peak of the CeO_2 doublet. A small peak coincides with the second peak of the CeO_2 doublet [curve (f)] indicating a small proportion of cerium in the +4 valence state. However, exposure to a corrosive environment converts all the cerium to the +4 valence state: curves (c) and (d) are identical to curve (f), the CeO_2 standard.

In alkaline solution, 4-valent cerium is thermodynamically stable (15). The formation of films containing 3-valent cerium indicates that the cerium was electroreduced at the surface during film formation. This shows the mechanism of formation of cerium-rich films on aluminum at open circuit and the dual role of oxygen. At cathodic areas on the surface, the pH increases due to oxygen reduction. This then facilitates the oxidation by the oxygen of 3-valent cerium to the 4-valent state in the solution. The 4-valent cerium is then electroreduced to a 3-valent cerium oxide/hydroxide

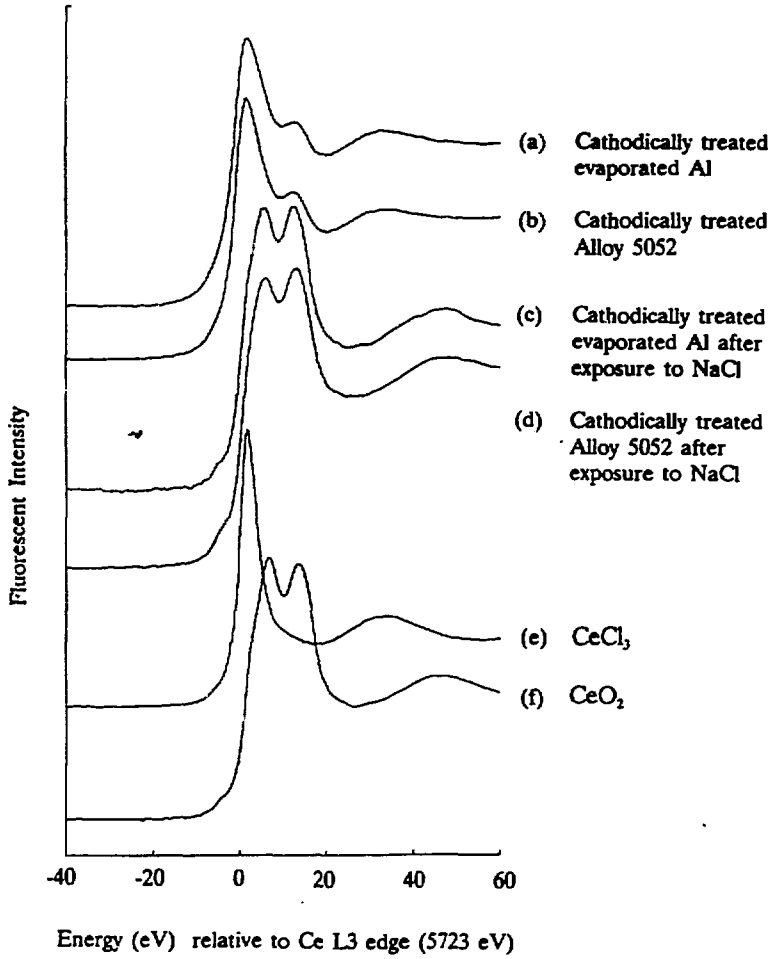

Fig. 4. Ce L3 x-ray absorption edge of cerium-containing oxide films on aluminum measured in fluorescence geometry with an incident angle of 4 mrad. (a) cathodically treated Al evaporated on glass, (b) cathodically treated Al Alloy 5052, (c) cathodically treated evaporated Al after immersion in NaCl, (d) cathodically treated Al Alloy 5052 after immersion in NaCl, (e) $CeCl_3.7H_2O$ (transmission), (f) CeO_2 (transmission).

film on the surface. This film appears to be electronically insulating, thus inhibiting further cathodic reaction. Evidence for the electronically insulating nature of the film is given by the conversion of 3-valent to 4-valent cerium on prolonged exposure of the film to NaCl solution. The open circuit potential of these specimens, -0.8 V(SCE), is well below the equilibrium between $Ce(OH)_3$ and CeO_2, indicating that conversion of the film to CeO_2 can only take place if there is no electronic connection to the metal. These results illustrate in detail the mechanism of cathodic inhibition of aluminum by cerium ions. They further illustrate an important principle of inhibition which is common to both chromates and cerium ions: the requirement of the presence of a soluble species which is converted to an insoluble form in the oxide film only at the oxide/solution interface.

ACKNOWLEDGMENTS

The measurements were made at the X11A Beam Line at the National Synchrotron Light Source at Brookhaven National Laboratory. We acknowledge the support of the U.S Department of Energy, Division of Materials Sciences, under Contract No. DE-AS05-80-ER10742 for its role in the development and operation of Beam Line X11 at the NSLS. This work was performed under the auspices of the U.S. Department of Energy, Division of Materials Sciences, Office of Basic Energy Sciences under Contract No. DE-AC02-76CH00016.

REFERENCES

1. M. Koudelkova, J. Augustynski, and H. Berthou, J. Electrochem. Soc. 124, 1165 (1977).
2. A. Kh. Bairamow, S. Zakipour, and C. Leygraf, Corros. Sci. 25, 69 (1985).
3. J. K. Hawkins, H. S. Isaacs, S. M. Heald, J. Tranquada, G. E. Thompson, and G. C. Wood, Corros. Sci. 27, 391 (1987).
4. S. M. Heald, E. Keller, and E. A. Stern, Phys. Lett. A 103, 155 (1984).
5. M. F. Abd Rabbo, J. A. Richardson, and G. C. Wood, Corros. Sci. 16, 689 (1976).
6. H. S. Isaacs, A. J. Davenport, S. M. Heald, H. Chen, and G. E. Thompson, to be published.
7. L. G. Parratt, Phys. Rev. 95, 359 (1954).
8. A. L. Hanson and H. S. Isaacs, unpublished results.
9. D. R. Arnott, B. R. W. Hinton, and N. E. Ryan, Corrosion 45, 12 (1989).
10. B. R. W. Hinton, Corrosion 89, New Orleans, Paper No. 170, NACE (1989).
11. F. Mansfeld, S. Lin, S. Kim, and H. Shih, Corros. Sci. 27, 997 (1987).
12. D. R. Arnott, N. E. Ryan, B. R. W. Hinton, B. A. Sexton, and A. E. Hughes, Appl. Surf. Sci. 22/23, 236 (1985).
13. T. K. Sham, J. Chem. Phys. 79, 1116 (1983).
14. A. J. Davenport, H. S. Isaacs, and M. W. Kendig, J. Electrochem. Soc. 136, 1837 (1989).
15. M. Pourbaix, Atlas of Electrochemical Equilibria in Aqueous Solutions, p. 194, NACE (1974).

DISCLAIMER